Since January 2020 Elsevier has created a COVID-19 resource centre with free information in English and Mandarin on the novel coronavirus COVID-19. The COVID-19 resource centre is hosted on Elsevier Connect, the company's public news and information website.

Biomedicine & Pharmacotherapy 146 (2022) 112513

Contents lists available at ScienceDirect

Biomedicine & Pharmacotherapy

journal homepage: www.elsevier.com/locate/biopha

In vitro interaction of potential antiviral TMPRSS2 inhibitors with human serum albumin and cytochrome P 450 isoenzymes

Erzsébet Pászti-Gere [a,*], Anna Szentkirályi [a], Zsófia Fedor [a], Gábor Nagy [a], Zoltán Szimrók [a], Zoltán Pászti [b], Anna Pászti [a], Oliver Pilgram [c], Torsten Steinmetzer [c], Slávka Bodnárová [d,e], Eszter Fliszár-Nyúl [d,e], Miklós Poór [d,e,**]

[a] Department of Pharmacology and Toxicology, University of Veterinary Medicine, István utca 2, Budapest H-1078, Hungary
[b] Institute of Materials and Environmental Chemistry, Research Centre for Natural Sciences, Magyar tudósok körútja 2, Budapest H-1117, Hungary
[c] Institute of Pharmaceutical Chemistry, Faculty of Pharmacy, Philipps University Marburg, Marbacher Weg 6-10, Marburg 35037, Germany
[d] Department of Pharmacology, Faculty of Pharmacy, University of Pécs, Rókus u. 2, Pécs H-7624, Hungary
[e] Lab-on-a-Chip Research Group, János Szentágothai Research Centre, University of Pécs, Ifjúság útja 20, Pécs H-7624, Hungary

ARTICLE INFO

Keywords:
3-amidinophenylalanine
Trypsin-like serine proteases
TMPRSS2
SARS-CoV-2, human serum albumin
Cytochrome P450 enzymes

ABSTRACT

The interactions of four sulfonylated Phe(3-Am)-derived inhibitors (MI-432, MI-463, MI-482 and MI-1900) of type II transmembrane serine proteases (TTSP) such as transmembrane protease serine 2 (TMPRSS2) were examined with serum albumin and cytochrome P450 (CYP) isoenzymes. Complex formation with albumin was investigated using fluorescence spectroscopy. Furthermore, microsomal hepatic CYP1A2, 2C9, 2C19 and 3A4 activities in presence of these inhibitors were determined using fluorometric assays. The inhibitory effects of these compounds on human recombinant CYP3A4 enzyme were also examined. In addition, microsomal stability assays (60-min long) were performed using an UPLC-MS/MS method to determine depletion percentage values of each compound. The inhibitors showed no or only weak interactions with albumin, and did not inhibit CYP1A2, 2C9 and 2C19. However, the compounds tested proved to be potent inhibitors of CYP3A4 in both assays performed. Within one hour, 20%, 12%, 14% and 25% of inhibitors MI-432, MI-463, MI-482 and MI-1900, respectively, were degraded. As essential host cell factor for the replication of the pandemic SARS-CoV-2, the TTSP TMPRSS2 emerged as an important target in drug design. Our study provides further preclinical data on the characterization of this type of inhibitors for numerous trypsin-like serine proteases.

1. Introduction

Type II transmembrane trypsin-like serine proteases (TTSPs) including the human airway trypsin-like protease (HAT)/ differentially expressed in squamous cell carcinoma (DESC), the hepsin/transmembrane protease serine (TMPRSS), the matriptase and the corin subfamilies are responsible for the activation or degradation of numerous proteins. Due to its involvement in the activation of the SARS-CoV-2 spike (S) protein, the TTSP TMPRSS2 in particular has come into the focus of numerous studies during the last few months. Similarly to other TTSPs, it contains an extracellularly located C-terminal serine protease domain as well as a stem region containing a group A scavenger receptor cysteine-rich domain (SRCR) and a low-density lipoprotein receptor class A domain (LDLRA) [1-3].

TMPRSS2 has also been described as a potential target in the treatment of seasonal flu, because proteolytic cleavage of influenza virus hemagglutinin (HA) by host cell proteases is a requirement for virus replication. Knockout of TMPRSS2 could strongly suppress the spread of H1N1 and H7N9 viruses into the lungs of mice; however, it has little effect on H3N2 infections [4,5]. Cleavage of spike protein (S) of SARS-CoV and MERS-CoV is accomplished by cellular serine proteases such as furin and TMPRSS2 and this proteolytic priming contributes greatly to viral entry into target cells thus propagation of infectivity in the host [6,7].

The novel severe acute respiratory syndrome coronavirus-2 (SARS-CoV-2), caused coronavirus disease 2019 (COVID-19), has become a global public health challenge recently (more than 257 million confirmed global cases and 5.1 million deaths until November, 2021;

* Corresponding author.
** Corresponding author at: Department of Pharmacology, Faculty of Pharmacy, University of Pécs, Rókus u. 2, Pécs H-7624, Hungary.
E-mail addresses: gere.erzsebet@univet.hu (E. Pászti-Gere), poor.miklos@pte.hu (M. Poór).

https://doi.org/10.1016/j.biopha.2021.112513
Received 22 September 2021; Received in revised form 24 November 2021; Accepted 6 December 2021
Available online 13 December 2021

https://covid19.who.int). Despite numerous successful vaccine developments, there is an urgent demand to develop efficient antiviral drugs, which have to be further characterized in appropriate animal models. The resistance of mice to SAR-CoV-2 can be eliminated via exogenous delivery of human angiotensin-converting enzyme 2 (ACE2) with a replication-deficient adenovirus (Ad5-hACE2). This murine model is suited for in vivo investigation of COVID-19 pathogenesis and to assess the efficacy of new or repurposed drugs against SARS-CoV-2 infections [8,9]. TMPRSS2 was reported to be co-expressed with the SARS-CoV receptor ACE2 on type II pneumocytes suggesting that proteolytic processing of S protein via TMPRSS2 function can regulate viral replication and spread in infected host [10,11]. Recent studies suggest that S protein of SARS-CoV-2 is proteolytically processed at two sites (S1/S2 and S2') by host-derived proteases [12-14]. In Calu-3 cells, furin cleaves the S protein at its S1/S2 site and TMPRSS2 at the S2′ site, thereby liberating the S2 subunit with its N-terminal fusion peptide, which enables the fusion of viral and cellular membranes. The involvement of these cellular serine proteases in the viral replication cycle makes these enzymes promising drug targets to block virus-host cell membrane fusion, and thus cellular entry of SARS-CoV-2 [15].

One strategy for drug design is the repurposing of already authorized serine protease inhibitors such as camostat mesylate (applied in the therapy of pancreatitis in Japan), gabexate mesylate (FOY), or nafamostat mesylate (an investigational drug regarding the treatment of COVID-19; ClinicalTrials.gov). There are promising in vitro results with nafamostat mesylate, as it could block successfully the S protein-mediated fusion and SARS-CoV-2 into human lung epithelium-derived Calu-3 cells [13,14,16]. In the same in vitro model, SARS-CoV-2 titers decreased in a dose-dependent manner after treatment with the Phe (3-Am)-derived inhibitors MI-432 and MI-1900, most likely via the suppression of TMPRSS2 [12]. These results suggest that inhibitors of trypsin-like serine proteases such as TMPRSS2 could be potential drugs for the treatment of SARS-CoV-2 infections. Therefore, the characterization of the Phe(3-Am)-type inhibitors, including the assessment of their drug interaction potential and biotransformation pathways, is of high interest.

Human serum albumin (HSA) is the most abundant plasma protein in the human circulation. It maintains the oncotic pressure and has antioxidant, buffer, and enzymatic functions in the blood [17]. In addition, HSA can entrap certain drugs and xenobiotics in the intravascular space, thereby affecting the tissue distribution of these compounds and/or their elimination rate [18]. Cytochrome P450 (CYP) isoenzymes are heme-containing proteins playing a key role in the biotransformation of numerous endogenous molecules, drugs, and xenobiotics in microsomes [19]. Both, the inhibition and induction of CYP enzymes, can significantly influence the pharmacokinetic behavior of numerous drugs, which are biotransformed by these proteins [20].

In this study, we evaluated the interactions of four sulfonylated Phe (3-Am)-derivatives (Fig. 1) with HSA and four CYP enzymes. Albumin-ligand interactions were investigated with fluorescence spectroscopy, while the inhibitory effect of these compounds on CYP enzymes was examined in human hepatic microsomes and employing the CypExpress CYP3A4 kit. In addition, depletion rates of the compounds were quantified in 60-min long microsomal stability assays by an UPLC-MS/MS method.

2. Materials and methods

2.1. Reagents

All reagents were analytical or HPLC grade. Inhibitors MI-432, MI-463, MI-482 and MI-1900 were synthesized as it has been reported [21]. Human serum albumin (HSA), racemic warfarin, CypExpress™ 3A4 Cytochrome P450 human kit, testosterone, 6β-hydroxytestosterone and ketoconazole were purchased from Merck (Darmstadt, Germany). To mimic extracellular physiological conditions, fluorescence spectroscopic measurements were performed in phosphate-buffered saline (PBS; 8.00 g/L NaCl, 0.20 g/L KCl, 1.81 g/L Na_2HPO_4 x 2 H_2O, 0.24 g/L KH_2PO_4; pH 7.4).

2.2. Spectroscopic studies

Fluorescence emission and UV–vis absorption spectra were recorded at 25 °C applying a Hitachi F-4500 fluorescence spectrophotometer (Tokyo, Japan) and a Jasco-V730 UV–vis spectrophotometer (Tokyo, Japan), respectively. The inner-filter effects of the inhibitors were corrected in each experiment, as described previously [22,23].

In quenching studies, we recorded the fluorescence emission spectrum of HSA (2 μM; λ_{ex} = 295 nm) without and with the ligands examined (0–10 μM) in PBS (pH 7.4). Changes in the emission signal of HSA were evaluated at 340 nm [24,25].

Furthermore, we tested the displacing ability of the protease inhibitors vs. the Sudlow's site I marker warfarin. Since the complex formation of warfarin with HSA strongly increases the emission signal of

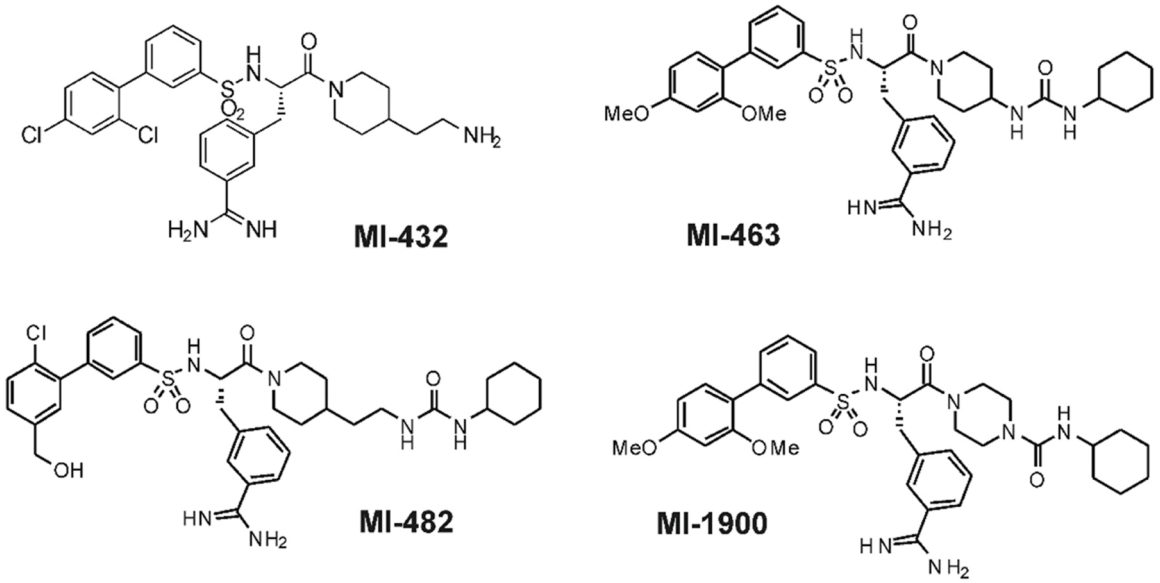

Fig. 1. Chemical structures of the examined Phe(3-Am)-derived inhibitors [21].

the site marker, the decrease in its emission intensity indicates the displacement of warfarin from the protein [24,25]. Therefore, increasing amounts of the inhibitors (final concentrations: 0–10 μM) were added to standardized warfarin and HSA concentrations (1 μM and 3.5 μM, respectively), then emission spectra of these samples were recorded (λ_{ex} = 317 nm). Changes in the emission signal of warfarin were evaluated at 379 nm.

2.3. Application of the Phe(3-Am)-derived inhibitors in microsomal activity and stability assays

Stock solutions of the inhibitors were prepared in dimethylsulfoxide (DMSO) and kept at − 20 °C, working solutions were prepared freshly from the stock solutions by dilution with the appropriate buffers prior to each experiment. After incubation of the microsomes with the inhibitors at 37 °C (using untreated samples as controls), the solutions were subjected to the subsequent fluorometric or UPLC/MS-MS procedures.

2.4. Effects on CYP activity of human liver microsomes

The Biovision CYP assays (BioVision, Inc, Kampenhout, Belgium) utilize non-fluorescent CYP1A2, 2C9, 2C19, or 3A4 substrates capable of transforming into a detectable highly fluorescent metabolite. In these experiments, α-naphthoflavone (α-NF; CYP1A2, 6 μM), tienilic acid (TA; CYP2C9, 60 μM), (+)-N-3-benzylnirvanol (BN; CYP2C19, 30 μM), and ketoconazole (CYP3A4, 30 μM) were used as inhibitors.

Preparation of suspensions for purchased human hepatic microsomes (Gibco, Biocenter, Szeged, Hungary, protein concentration: 20 mg/mL) were made separately by mixing 25 μL with 2425 μL assay buffer and with 50 μL NADPH generating system (100 ×). Aliquots of 50 μL microsomal suspensions were treated with the protease inhibitors (each 20 μL, 0–250 μM, except MI-1900 where the maximal concentration was 50 μM), known reference inhibitors (each 20 μL; α-naphthoflavone, 30 μM; tienilic acid, 300 μM; (+)-N-3-benzylnirvanol, 150 μM; ketoconazole, 150 μM), or 20 μL assay buffer without test compounds as background control for 15 min at 37 °C (in CYP2C19 assay, 30 min incubation was applied), after which 30 μL of the appropriate CYP substrate/$NADP^+$ mixture was added to each well yielding a final reaction volume of 100 μL/well.

The protein content of the obtained microsomes was determined using the bicinchoninic acid protein assay kit (Pierce BCA kit, Thermo Fisher Scientific, Waltham, MA, US). The final microsomal protein concentration was 10 μg/well in each assay. The used solvents (≤ 0.5% DMSO and ≤ 1% acetonitrile) did not cause any significant inhibition of CYP enzymes examined.

The fluorescence intensities were measured with a fluorometer (Victor X2 2030, Perkin Elmer, Waltham, MA, US) using $\lambda_{ex/em}$= 406/468 nm for CYP1A2, $\lambda_{ex/em}$= 415/502 nm for CYP2C9, $\lambda_{ex/em}$= 406/468 nm for CYP2C19, and $\lambda_{ex/em}$= 535/587 nm for CYP3A4 assays. IC_{50} values were determined by sigmoidal fitting using the OriginPro8 software (OriginLab Corporation; Northampton, MA, US).

2.5. Effects on CYP3A4-catalyzed testosterone oxidation

The inhibitory effect of the protease inhibitors on CYP3A4 was also examined employing testosterone, a FDA-recommended substrate. Incubations were performed using CypExpress™ 3A4 Cytochrome P450 human kit as described previously, without modificantions [26,27].

After incubation, testosterone and its metabolite (6β-hydroxytestosterone) were quantified by HPLC. The integrated HPLC system (Jasco, Tokyo, Japan) used was built up of an autosampler (AS-4050), a binary pump (PU-4180), and an UV-Vis detector (UV-975). Chromatograms were evaluated with the ChromNAV software.

The protease inhibitors were analyzed with the previously reported HPLC method [26,27] using minor modifications. Samples injected (20 μL) were driven through a Phenomenex Security Guard column (C18, 4.0 × 3.0 mm) linked to a Kinetex EVO-C18 (150 × 4.6 mm, 5 μm; Phenomenex, Torrance, CA, US) analytical column. Isocratic elution was performed using 1.2 mL/min flow rate at room temperature. Testosterone and its hydroxylated metabolite were detected at 240 nm. Regarding inhibitors MI-432, MI-463, and MI-1900, the mobile phase consisted of methanol, water, and acetic acid (53:46:1 v/v%). Since compound MI-482 was co-eluted with 6β-hydroxytestosterone, a modified mobile phase was applied, which contained sodium acetate buffer (6.9 mM, pH 4.0) and acetonitrile (65:35 v/v%; other experimental conditions were the same as above).

Each experiment was performed at least in triplicates, the results are provided as mean ± SD values. IC_{50} values of the inhibitors were determined by sigmoidal fitting using the OriginPro8 software (OriginLab Corporation; Northampton, MA, US).

2.6. UPLC-MS/MS method for the determination of the inhibitor degradation

Human liver microsomes (Gibco, Biocenter, Szeged, Hungary, final concentration after dilution: 1 mg/mL) were exposed to the four protease inhibitors at 50 μM for 60 min. The reaction buffer (100 mM phosphate buffer, pH 7.4) contained 1 mM NADPH, 5 mM $MgCl_2$, 10 mM glucose-6-phosphate, and 2 IU/mL glucose-6-phosphate dehydrogenase. The reaction was stopped with a two-fold volume of ice-cold acetonitrile. Samples were centrifuged for 10 min at 10,000 g at room temperature, then the supernatants were directly analyzed by UPLC-MS/MS. Controls without human microsomes were also tested. In the absence of CYP enzymes, the decomposition rates of the inhibitors were less than 0.5%. All experiments were performed in triplicates. The rates of metabolic degradation were determined for each inhibitor applied.

Determination of analytes was carried out using an UPLC/MS/MS system, which consisted of an HPLC (SCIEX ExionLC™ UPLC, Framigham, Massachusetts, US) including a SCIEX ExionLC™ AD controller, a binary SCIEX ExionLC™ pump and a SCIEX ExionLC™ degasser, and a SCIEX Qtrap 4500 triple-quadrupole mass spectrometer (Framigham, Massachusetts, US) equipped with SCIEX Turbo V electrospray ionization source. The HPLC columns used were LiChrospher RP Select B (125 × 4.0 mm, 5.0 μm, C8). For chromatographic separation, trifluoroacetic acid (0.1%) in ultrapurified water (A) and acetonitrile (B) were used as the components of the mobile phase, applying a gradient elution. The gradient program was the following: between 0 and 10 min 70% A and 30% B, from 10 to 20 min linear increase to 50% A and 50% B, from 20 to 21 min keeping at 50% A and 50% B, from 21 to 22 min linear change to 70% A and 30% B, and from 22 to 30 min kept 70% A and 30% B. The run time was 30 min, column temperature was adjusted to 35 °C, the flow rate was 1.0 mL/min.

The ion transitions shown in Table 1 are of two varieties. The bolded ones are the quantifier ions, which are the primary identifiers of the compounds they belong to and are used in quantification calculations. The non-bolded ones are called qualifier ions, which prove that the peak belonging to the quantifier is derived from impurities or another compound. Since compounds having low mass to charge fragments, it was prudent to place one more qualifier ion to each. The ion source and ion focus conditions were the followings: curtain gas (N_2): 40 psi, ion source potential: 5500 V, ion source temperature: 650 °C, source gas (N_2): 40 psi. The entrance potential is either + 10 V or −10 V depending to the ionization mode.

2.7. Statistical analyses

For statistical evaluation, the R 2.11.1 software package (2010) was applied (*$p < 0.05$, **$p < 0.01$, ***$p < 0.001$). Differences between absolute means were evaluated by one-way analysis of variance (one-way ANOVA) with post-hoc Tukey test, where data were of normal distribution and homogeneity of variances was confirmed.

Table 1
The optimised multiple reaction monitoring (MRM) transitions and values (bold: quantifier ion). Q_1/Q_3 mass – the mass per charge ratio (molecule-ion mass) let through the first/third quadrupole.

Q_1 mass / Da	Q_3 mass / Da	Dwell time / msec	Identifier	Declustering potential / V	Collision energy / V	Collision cell exit potential / V
601.990	**186.0**	**80**	**MI-432-1**	**166**	**95**	**12**
601.990	117.0	80	MI-432-2	166	131	8
601.990	112.0	80	MI-432-3	166	59	8
676.991	**198.1**	**80**	**MI-1900-1**	**181**	**93**	**8**
676.991	182.9	80	MI-1900-2	181	133	12
676.991	117.0	80	MI-1900-3	181	145	18
691.117	117.0	80	MI-463 1	101	143	8
691.117	183.0	80	MI-463 2	101	131	12
691.117	**198.0**	**80**	**MI-463 3**	**101**	**97**	**8**
723.118	112.0	80	MI-482 1	156	105	8
723.118	117.0	80	MI-482 2	156	169	10
723.118	**152.0**	**80**	**MI-482 3**	**156**	**157**	**10**

3. Results

3.1. Interaction of the inhibitors with HSA

To test the potential interactions of the protease inhibitors with HSA, fluorescence quenching studies were performed. Under the applied conditions, the ligands caused only a minor decrease in the emission signal of HSA (Fig. 2A), without statistically significant effects ($p < 0.05$). Among the examined compounds, inhibitor MI-482 induced the largest (approximately 8%) decrease. These observations suggest negligible or weak interactions of these ligands with the HSA.

To confirm the results of quenching studies, the displacing ability of the four inhibitors vs. the Sudlow's site I marker warfarin was also examined. In agreement with quenching experiments, the inhibitors MI-432, MI-463, and MI-1900 did not modify significantly the emission signal of warfarin, while compound MI-482 caused a slight but statistically significant decrease (approximately 10% at 10 μM concentration; Fig. 2B). Therefore, it is reasonable to hypothesize that inhibitor MI-482 forms poorly stable complex with HSA, and the affinity of analogues MI-432, MI-463, and MI-1900 toward this protein is even lower.

3.2. Inhibitory effects on CYP1A2, 2C9, 2C19, and 3A4

Since inhibitor MI-1900 possessed autofluorescence at higher concentrations (explaining the elevation in fluorescence intensities when exposed with microsomes), it was only used up to 10 μM for IC_{50} determination (Fig. 3). However, none of the compounds inhibited human microsomal CYP1A2, 2C9 and 2C19 (Fig. 4).

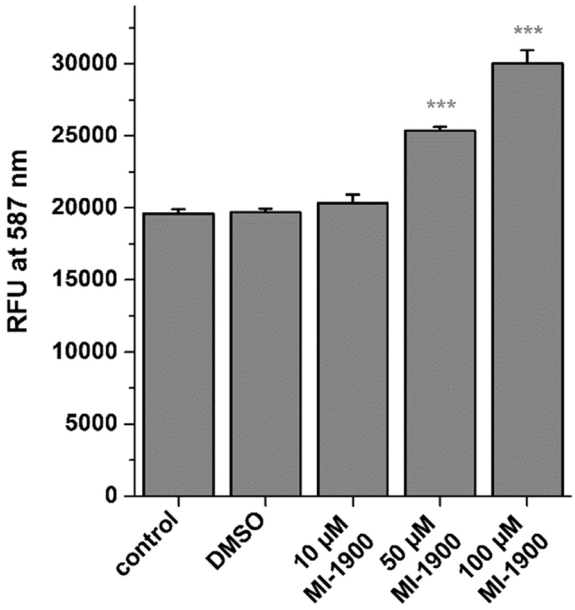

Fig. 3. Autofluorescence signals produced by inhibitor MI-1900 (10, 50 and 100 μM) in absence of CYP3A4 ($\lambda_{ex/em}$=535/587 nm). Data are presented as means ± SD (***$p < 0.001$; $n = 3$).

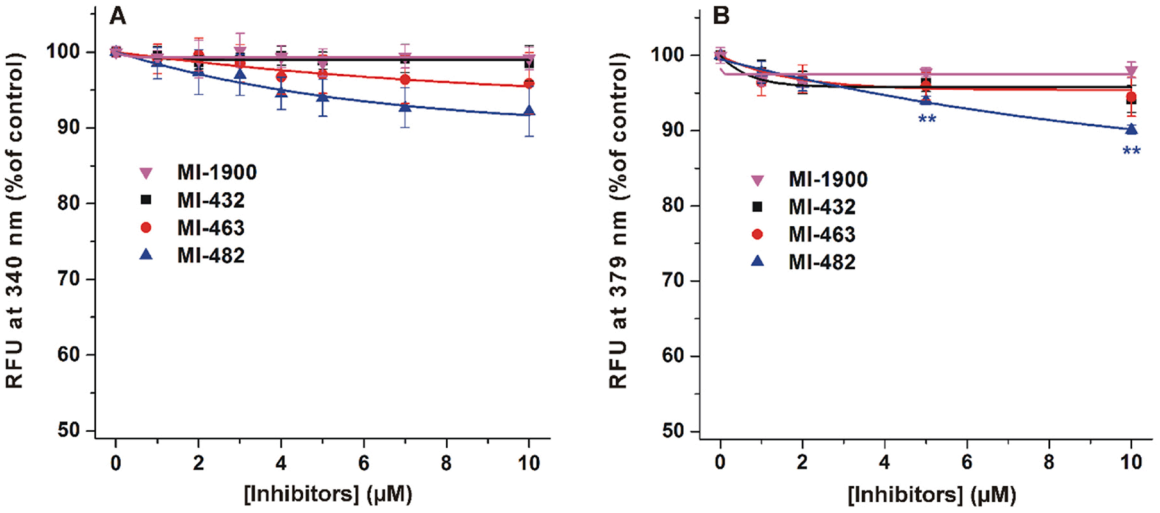

Fig. 2. Relative changes in the fluorescence emission signal of HSA (A; 2.0 μM, $\lambda_{ex} = 295$ nm, $\lambda_{em} = 340$ nm) and warfarin-HSA system (B; 1.0 μM warfarin, 3.5 μM HSA, $\lambda_{ex} = 317$ nm, $\lambda_{em} = 379$ nm) in the presence of increasing inhibitor concentrations (0–10 μM) in PBS (pH 7.4; **$p < 0.01$; $n = 3$).

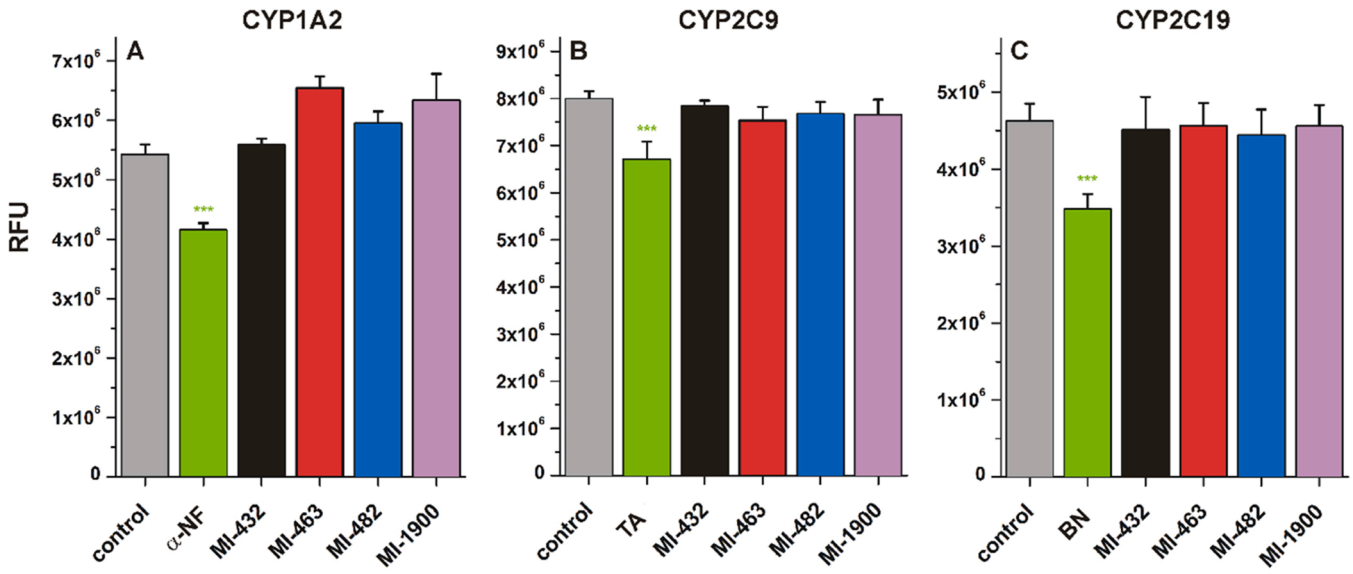

Fig. 4. Lack of inhibitory effects of the protease inhibitors on CYP1A2 (A), CYP2C9 (B) and CYP2C19 (C) activities. The reference compound α-naphthoflavone (α-NF) at 6 μM suppressed significantly CYP1A2 function (***$p < 0.001$); however, neither of the protease inhibitors at 50 μM altered CYP1A2 activity in human hepatic microsomes. The reference compounds tienilic acid (TA) at 60 μM and (+)-N-3 benzylnirvanol (BN) at 30 μM inhibited the functions of CYP2C9 and CYP2C19, respectively (***$p < 0.001$). In contrast, the protease inhibitors did also not affect CYP2C9 and CYP2C19 activities. Fluorescence intensity data ($\lambda_{ex}/_{em}$=406/468 nm for CYP1A2, $\lambda_{ex}/_{em}$=415/502 nm for CYP2C9, $\lambda_{ex}/_{em}$=406/468 nm for CYP2C19) are presented as means ± SD (n = 3).

However, each substance showed strong, concentration-dependent inhibitory effects on the human microsomal CYP3A4 isoenzyme (Fig. 5A). Inhibitor MI-463 (IC_{50} = 0.21 ± 0.03 μM) proved to be the most potent among the tested compounds, followed by analogues MI-482 (IC_{50} = 0.30 ± 0.07 μM), MI-432 (IC_{50} = 0.39 ± 0.09 μM) and MI-1900 (IC_{50} = 0.63 ± 0.04 μM).

The inhibitory effect on CYP3A4 was also tested employing the FDA-recommended substrate testosterone using the CypExpress™ 3A4 Cytochrome P450 human kit. In agreement with the experiments performed on microsomes, each protease inhibitor caused a significant decrease in CYP3A4-catalyzed testosterone metabolite formation (Fig. 5B). In this assay, the strongest inhibitor was also compound MI-463 (IC_{50} = 2.0 ± 0.3 μM), followed by MI-482 (IC_{50} = 4.6 ± 0.6 μM), MI-1900 (IC_{50} = 6.2 ± 1.7 μM) and MI-432 (IC_{50} = 11.8 ± 2.3 μM).

3.3. Depletion of the protease inhibitors in microsomal preparations

Based on 60-min microsomal stability data, each protease inhibitor was decomposed during the exposure to hepatic microsomal CYP isoenzymes; however, this degradation occurred to different degrees (Fig. 6). Compounds MI-432 and MI-1900 were degraded to the highest extent. The depletion values were 20.2 ± 2.1%, 11.5 ± 3.6%, 14.3 ± 2.5% and 24.5 ± 6.7% for compounds MI-432, MI-463, MI-482 and MI-1900, respectively. Significant differences were found between the metabolization of inhibitors MI-1900 and MI-463 ($p = 0.0099$), as well as between the degradation of compounds MI-1900 and MI-482 ($p = 0.0418$).

4. Discussion

Despite the rapid development of various highly effective vaccines for the prevention of SARS-CoV-2 infections, no efficient antiviral

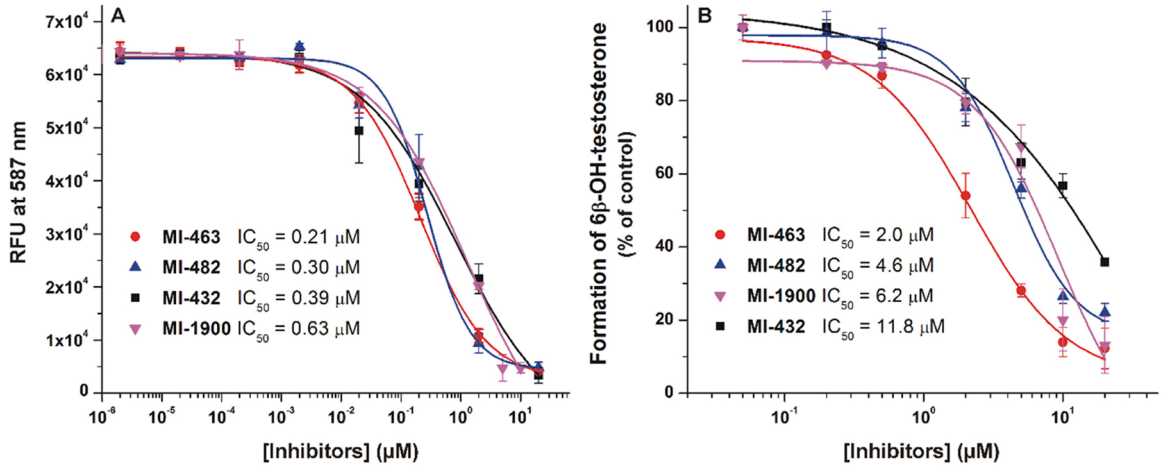

Fig. 5. (A) Effects of the tested inhibitors on human microsomal CYP3A4 activity (incubation: 15 min, 37 °C, with 10 μg/well protein content). **(B)** Reduction of the CYP3A4-catalyzed 6β-hydroxytestosterone formation by the used protease inhibitors. The IC_{50} value of the positive control ketoconazole was 0.2 μM. Data represent mean values ± SD (n = 3).

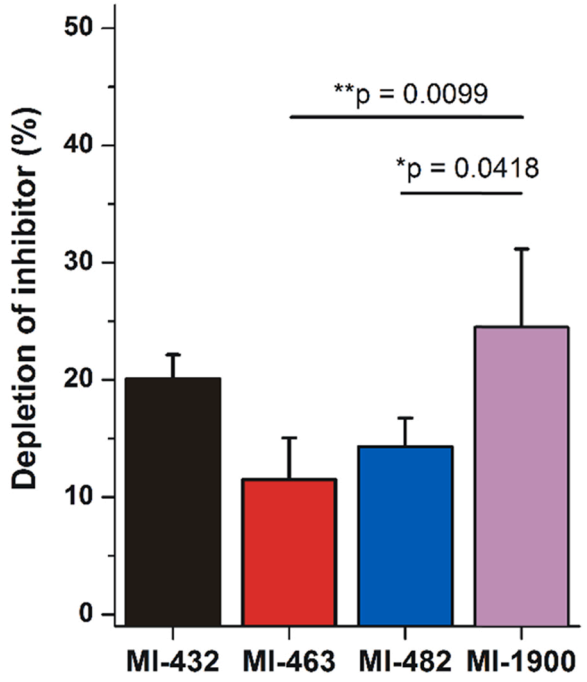

Fig. 6. Depletion % of the protease inhibitors (50 μM) after 60 min incubation with a human microsomal preparation. The human microsome concentration in assay buffers was 1 mg/mL. The highest degradation was observed for inhibiotr MI-1900, which significantly differed from that of analogues MI-463 (**p =0.0099) and MI-482 (*p = 0.0418). Data are represented as mean ± SDs (n = 3). In each control sample, the degradation rate was negligible (less than 0.015%).

therapeutical alternatives are available so far in COVID-19 patients. Repurposing of already authorized (antiviral) drugs could be a possible treatment option to reduce viral infectivity and spread. These pharmacological strategies can include blockage of virus entry via targeting the SARS-CoV-2 spike protein (FOY, nafamostat and camostat mesylate), application of nucleotide analogues addressing the viral RNA-dependent RNA polymerase (such as favipiravir, ribavirin, remdesivir and galidesivir), or suppression of the SARS-CoV-2 proteases (e.g. lopinavir/ritonavir, nelfinavir and danoprevir) [15]. The high-throughput x-ray crystallographic screen of two repurposing drug libraries against an interesting drug target for coronaviruses, M^{pro} revealed that 37 already-approved drugs and drugs in clinical trials could bind to this SARS-CoV-2 protease and among them one peptidomimetic and six nonpeptidic compounds showed antiviral activity at nontoxic concentrations in vitro [28]. M^{pro} can also be blocked by novel α-ketoamide inhibitor having P3-P2 amide bond incorporated into a pyridone ring to enhance the half-life of the compound suitable for inhalation adminsitration route [29]. In addition, several COVID-19 studies imply trials with inhibitors of the host cell protease TMPRSS2 such as camostate and nafamostate mesylate or FOY 305 even in combination with other antiviral agents (ClinicalTrials.gov). However, these compounds are relatively unselective inhibitors of numerous trypsin-like serine proteases and possess a relatively short half-life.

Therefore, the development of improved more selective TMPRSS2 inhibitors with a better safety profile could be a promising strategy for more efficient SARS-CoV-2 treatments. TMPRSS2 seems to be modulated by androgens supporting the assumption that there might be differences in COVID-19 infection in male and female patients due to the variations in androgen levels. Antiandrogen agents such as enzalutamide could also reduce TMPRSS2 activity by decreasing the expression of this TTSP. However, after treatment with enzalutamide SARS-COV-2 infection was suppressed mainly in human prostate cells and not in human lung cells indicating that TMPRSS2 expression might be androgen receptor independent in human lung epithelial cells [8]. However, there may be still a rationale for the application of androgen receptor-modulating drugs or coregulators such as bromodomain and extra-terminal domain (BET) inhibitors in COVID-19 therapy for decreasing TMPRSS2 expression.

Until now, several more efficient serine protease inhibitors were developed including the sulfonylated Phe(3-Am)-derivatives [21,30] and the substrate-analogue ketobenzothiazole derivatives originated from the known P4-P1 Arg-Gln-Ala-Arg substrate sequence at the autocatalytic activation site of matriptase [31]. Within the series of the Phe(3-Am) analogues, the dibasic derivative MI-432 possessing an N-terminal dichloro-substituted biphenyl-3-sulfonyl group and a C-terminal aminoethylpiperidide moiety was one of the most potent matriptase inhibitors. Typically, Phe(3-Am)-derived inhibitors in complex with trypsin-like serine proteases adopt a Y-shape conformation. Based on a modeled complex of MI-432 in matriptase it was found that the N-terminal biphenyl group of MI-432 appeared to fit into the S3/4 pocket of matriptase making contacts to the aromatic side chains of the characteristic TMPRSS2 residue Phe99, as well as to Trp215, the latter residue is found in most trypsin-like serine proteases. Modeling of this inhibitor type in TMPRSS2 suggested a very similar binding mode [32].

In previous studies, human lung epithelium-derived Calu-3 cells infected with H1N1 or H3N2 influenza viruses were treated with MI-432 and related potential TMPRSS2 inhibitors at a concentration of 50 μM. After 48 h, significantly reduced viral titers were observed when compared to controls in absence of inhibitors [30,33]. Furthermore, it has been recently demonstrated that the inhibitors MI-432 and MI-1900 prevented the replication and spread of the new SARS-CoV-2 in infected Calu-3 cells in a dose-dependent manner, most-likely via an inhibition of the membrane-bound host protease TMPRSS2 [12]. In our previous study, we demonstrated on human intestinal epithelial cells (HIEC) and on primary human hepatocytes (PHH) that MI-1900 and its structural close analogue MI-1907 (up to 50 μM) did not affect cell viability and did not elevate inflammatory responses (e.g. IL-6 and IL-8 production) [32]. Nevertheless, disturbances of redox status of PHH were observed after MI-1900 and MI-1907 treatment. This elevation in extracellular hydrogen peroxide levels was not detected in intestinal epithelial cells of human (HIEC) and porcine origins (IPEC-J2) [32,34].

For a better preclinical characterization of the used Phe(3-Am)-derived protease inhibitors, HSA binding studies and CYP isoenzyme activity measurements have been performed. Only a few CYP isoenzymes such as CYP1A2, 2C9, 2C19 and 3A4 are responsible for metabolizing the major part of authorized drugs [35]. This is the first study focusing on the interaction of these four Phe(3-Am)-derived inhibitors with serum albumin and hepatic CYP isoenzymes, two of these inhibitors also showed a significant antiviral effect on SARS-CoV-2 replication.

The Trp-214 amino acid is mainly responsible for the fluorescence signal of HSA [17]. Since the size of albumin is not too large (66.5 kDa), the complex formation of a ligand molecule can partially quench the fluorescence signal of the macromolecule, even if its binding site is not found in the Sudlow's site I region (subdomain IIA, where Trp-214 is located). Therefore, the fact that the used protease inhibitors induced only minor changes in the emission signal of HSA (Fig. 2A) indicated a weak interaction of these ligands with the protein. Inhibitor MI-482 was able to slightly decrease the albumin binding of the site I marker warfarin (Fig. 2B) suggesting a weak interacion with HSA, however, only low-affinity complexes are formed. These data suggest that neither albumin nor a biotransformation by the isoenzymes CYP1A2, 2C9 and 2C19 should have a significant influence on the pharmacokinetics of the tested inhibitors.

Based on both assays employing human microsomes or the recombinant enzyme (Fig. 5), the examined Phe(3-Am)-derivatives proved to be strong inhibitors of CYP3A4, causing significant inhibition at the nanomolar or low micromolar range. The IC_{50} values for CYP3A4 are in the range between 0.21 and 0.63 μM indicating that CYP3A4 may be

involved in their microsomal degradation. The depletion rates of compounds MI-432 and MI-1900 were approximately 20% at the end of the 60 min investigation period, while for analogues MI-463 or MI-482 a significantly reduced degradation has been observed (<15%). CYP3A4-catalyzed testosterone hydroxylation was also strongly inhibited by compounds MI-463, MI-482 and MI-1900 (IC_{50} = 2–6 μM), while the IC_{50} value of MI-432 exceeded 10 μM.

Until now, no in vivo PK data are available for the tested four protease inhibitors. A Phe(3-Am)-piperazide derivative possessing a similar structure like inhibitor MI-1900 was administered intavenously (1 mg/kg) in rats and a very rapid elimination was observed [36]. An established method to improve the oral bioavailability and to reduce the rapid elimination of such monobasic Phe(3-Am) derivatives, is the conversion of their amidino function into a hydroxyamidine [37]. The most advanced Phe(3-Am) protease inhibitor is mesupron, the hydroxyamidino prodrug of the amidine compound WX-UKI-1. It was found that this substance decayed in a mono-phasic pattern with a very short half-life after a single intravenous injection of 2 mg/kg in rats [38,39]. The hydroxyamidino prodrug is an intermediate during the final synthesis steps of the inhibitor, which is obtained during the conversion of the nitril group into an amidine group. It was observed that the prodrug itself possesses no inhibitory potency, thus the hydroxyamidino prodrugs of the used four inhibitors have not been further evaluated. Therefore, it can be only speculated that PK data for the prodrugs would be similar to those obtained in case of mesupron. The characterization of the PK properties of the potential hydroxyamidino prodrugs of the tested four inhibitors is, however, beyond the scope of this study. Herein, we demonstrate the results of an in vitro drug-drug interaction screening of these compounds before administration of them in experimental animals without animal sacrifice in accordance with 3Rs and animal welfare practice.

It should be stated that these inhibitors can also affect other trypsin-like serine proteases such as matriptases or clotting factors. Therefore, the development of more selective TMPRSS2 inhibitors would be beneficial for their use as antiviral agents, including the treatment of SARS-CoV-2 infections.

Funding

This work was supported by the Hungarian National Research, Development and Innovation Office under grant number 124522. This project was supported by the János Bolyai Research Scholarship of the Hungarian Academy of Sciences and by the ÚNKP-20-5 New National Excellence Program of the Ministry for Innovation and Technology from the source of the National Research, Development and Innovation Fund.

Contributions

EPG designed the study. GN and ZSZ performed the UPLC/MS-MS measurements during microsomal stability assays and interpreted the results. EPG and ZP carried out fluorometric experiments and evaluated data. OP and TS were responsible for inhibitor synthesis. EFN, SB and MP performed spectroscopic studies and CYP3A4 assay with testosterone substrate. Statistical analysis was made by EPG. EPG, TS and MP wrote the manuscript which was approved by the other authors.

CRediT authorship contribution statement

Erzsébet Gere-Pászti: Conceptualization, Methodology, Formal analysis, Writing – review & editing, Supervision, Project administration, **Anna Szentkirályi**: Investigation, Formal analysis, **Zsófia Fedor**: Investigation, Formal analysis, **Gábor Nagy**: Investigation, Validation, Formal analysis, Resources, **Zoltán Szimrók**: Investigation, Validation, Formal analysis, Resources, **Zoltán Pászti**: Investigation, Validation, Formal analysis, Visualization, **Anna Pászti**: Methodology, Investigation, **Oliver Pilgram**: Resources, Methodology, Writing – review & editing, **Torsten Steinmetzer**: Conceptualization, Writing – review & editing, Supervision, **Slávka Bodnárová**: Investigation, Validation, Formal analysis, **Eszter Fliszár-Nyúl**: Investigation, Validation, Formal analysis, **Miklós Poór**: Conceptualization, Methodology, Formal analysis, Writing – review & editing, Supervision, Project administration.

Ethics declaration

Animal experiments were not carried out during this study.

Conflict of interest statement

The work of this paper has been performed as independent scientific work with no interferences from any third party. The other authors declare that the research was conducted in the absence of any commercial or financial relationships that could be construed as a potential conflict of interest.

Acknowledgments

The authors would like to acknowledge the technical support of Eszter Varga (Department of Pharmacology and Toxicology, University of Veterinary Medicine, Budapest, Hungary) in fluorometric methods. The authors thank to Katalin Fábián (Department of Pharmacology, Faculty of Pharmacy, University of Pécs, Pécs, Hungary) for her excellent assistance in the experimental work.

References

[1] T.M. Antalis, T.H. Bugge, Q. Wu, Membrane-anchored serine proteases in health and disease, Prog. Mol. Biol. Transl. Sci. 99 (2011) 1–50, https://doi.org/10.1016/B978-0-12-385504-6.00001-4.

[2] J.D. Hooper, J.A. Clements, J.P. Quigley, T.M. Antalis, Type II transmembrane serine proteases. Insights into an emerging class of cell surface proteolytic enzymes, J. Biol. Chem. 276 (2001) 857–860, https://doi.org/10.1074/jbc.R000020200.

[3] R. Szabo, T.H. Bugge, Type II transmembrane serine proteases in development and disease, Int. J. Biochem. Cell Biol. 40 (2008) 1297–1316, https://doi.org/10.1016/j.biocel.2007.11.013.

[4] W. Garten, C. Braden, A. Arendt, C. Peitsch, J. Baron, Y. Lu, K. Pawletko, K. Hardes, T. Steinmetzer, E. Böttcher-Friebertshäuser, Influenza virus activating host proteases: identification, localization and inhibitors as potential therapeutics, Eur. J. Cell Biol. 94 (2015) 375–383, https://doi.org/10.1016/j.ejcb.2015.05.013.

[5] C. Tarnow, G. Engels, A. Arendt, F. Schwalm, H. Sediri, A. Preuss, P.S. Nelson, W. Garten, H.D. Klenk, G. Gabriel, E. Böttcher-Friebertshäuser, TMPRSS2 is a host factor that is essential for pneumotropism and pathogenicity of H7N9 influenza A virus in mice, J. Virol. 88 (2014) 4744–4751, https://doi.org/10.1128/JVI.03799-13.

[6] E. Böttcher-Friebertshäuser, Membrane-anchored serine proteases: host cell factors in proteolytic activation of viral glycoproteins, in: E. Böttcher-Friebertshäuser, W. Garten, H. Klenk (Eds.), Activation of Viruses by Host Proteases, Springer, Cham, 2018, pp. 153–203, https://doi.org/10.1007/978-3-319-75474-1_8.

[7] M. Hoffmann, H. Hofmann-Winkler, S. Pöhlmann, Priming time: how cellular proteases arm coronavirus spike proteins, in: E. Böttcher-Friebertshäuser, W. Garten, H. Klenk (Eds.), Activation of Viruses by Host Proteases, Springer, Cham, 2018, pp. 71–98, https://doi.org/10.1007/978-3-319-75474-1_4.

[8] F. Li, M. Han, P. Dai, W. Xu, J. He, X. Tao, Y. Wu, X. Tong, X. Xia, W. Guo, Y. Zhou, Y. Li, Y. Zhu, X. Zhang, Z. Liu, R. Aji, X. Cai, Y. Li, D. Qu, Y. Chen, S. Jiang, Q. Wang, H. Ji, Y. Xie, Y. Sun, L. Lu, D. Gao, Distinct mechanisms for TMPRSS2 expression explain organ-specific inhibition of SARS-CoV-2 infection by enzalutamide, Nat. Commun. 12 (2021) 866, https://doi.org/10.1038/s41467-021-21171-x.

[9] J. Sun, Z. Zhuang, J. Zheng, K. Li, R.L. Wong, D. Liu, J. Huang, J. He, A. Zhu, J. Zhao, X. Li, Y. Xi, R. Chen, A.N. Alshukairi, Z. Chen, Z. Zhang, C. Chen, X. Huang, F. Li, X. Lai, D. Chen, L. Wen, J. Zhuo, Y. Zhang, Y. Wang, S. Huang, J. Dai, Y. Shi, K. Zheng, M.R. Leidinger, J. Chen, Y. Li, N. Zhong, D.K. Meyerholz, P. B. McCray Jr., S. Perlman, J. Zhao, Generation of a broadly useful model for COVID-19 pathogenesis, vaccination, and treatment, Cell 182 (2020) 734–743, https://doi.org/10.1016/j.cell.2020.06.010 (e5).

[10] I. Glowacka, S. Bertram, M.A. Müller, P. Allen, E. Soilleux, S. Pfefferle, I. Steffen, T. S. Tsegaye, Y. He, K. Gnirss, D. Niemeyer, H. Schneider, C. Drosten, S. Pöhlmann, Evidence that TMPRSS2 activates the severe acute respiratory syndrome coronavirus spike protein for membrane fusion and reduces viral control by the humoral immune response. J. Virol. 85 (2011) 4122–4134, https://doi.org/10.1128/JVI.02232-10.

[11] E.C. Mossel, J. Wang, S. Jeffers, K.E. Edeen, S. Wang, G.P. Cosgrove, C.J. Funk, R. Manzer, T.A. Miura, L.D. Pearson, K.V. Holmes, R.J. Mason, SARS-CoV

replicates in primary human alveolar type II cell cultures but not in type I-like cells, Virology 372 (2008) 127–135, https://doi.org/10.1016/j.virol.2007.09.045.
[12] D. Bestle, M.R. Heindl, H. Limburg, T.V. Lam van, O. Pilgram, H. Moulton, D. A. Stein, K. Hardes, M. Eickmann, O. Dolnik, et al., TMPRSS2 and furin are both essential for proteolytic activation and spread of SARS-CoV-2 in human airway epithelial cells and provide promising drug targets, bioRxiv 9 (2020), e202000786, https://doi.org/10.26508/lsa.202000786.
[13] M. Hoffmann, S. Schroeder, H. Kleine-Weber, M.A. Müller, C. Drosten, S. Pöhlmann, Nafamostat, mesylate blocks activation of SARS-CoV-2: New treatment option for COVID-19, Antimicrob. Agents Chemother. 64 (6) (2020) e00754–20, https://doi.org/10.1128/AAC.00754-20.
[14] M. Hoffmann, H. Kleine-Weber, S. Schroeder, N. Krüger, T. Herrler, S. Erichsen, T. S. Schiergens, G. Herrler, N.H. Wu, A. Nitsche, et al., SARS-CoV-2 cell entry depends on ACE2 and TMPRSS2 and is blocked by a clinically proven protease inhibitor, Cell 8674 (2020) 30229–30234, https://doi.org/10.1016/j.cell.2020.02.052.
[15] R. Ghanbari, A. Teimoori, A. Sadeghi, A. Mohamadkhani, S. Rezasoltani, E. Asadi, A. Jouyban, S.C. Sumner, Existing antiviral options against SARS-CoV-2 replication in COVID-19 patients, Future Microbiol. 15 (2020) 1747–1758, https://doi.org/10.2217/fmb-2020-0120.
[16] M. Yamamoto, M. Kiso, Y. Sakai-Tagawa, K. Iwatsuki-Horimoto, M. Imai, M. Takeda, N. Kinoshita, N. Ohmagari, J. Gohda, K. Semba, Z. Matsuda, Y. Kawaguchi, Y. Kawaoka, J.I. Inoue, The anticoagulant nafamostat potently inhibits SARS-CoV-2 S protein-mediated fusion in a cell fusion assay system and viral infection in vitro in a cell-type-dependent manner, Viruses 12 (6) (2020) 629, https://doi.org/10.3390/v12060629.
[17] G. Fanali, A. di Masi, V. Trezza, M. Marino, M. Fasano, P. Ascenzi, Human serum albumin: from bench to bedside, Mol. Asp. Med. 33 (2012) 209–290, https://doi.org/10.1016/j.mam.2011.12.002.
[18] K. Yamasaki, V.T. Chuang, T. Maruyama, M. Otagiri, Albumin-drug interaction and its clinical implication, Biochim. Biophys. Acta 1830 (2013) 5435–5443, https://doi.org/10.1016/j.bbagen.2013.05.005.
[19] B. Meunier, S.P. de Visser, S. Shaik, Mechanism of oxidation reactions catalyzed by cytochrome P450 enzymes, Chem. Rev. 104 (2004) 3947–3980, https://doi.org/10.1021/cr020443g.
[20] J. Hakkola, J. Hukkanen, M. Turpeinen, O. Pelkonen, Inhibition and induction of CYP enzymes in humans: an update, Arch. Toxicol. 94 (2020) 3671–3722, https://doi:10.1007/s00204-020-02936-7.
[21] M. Hammami, E. Rühmann, E. Maurer, A. Heine, M. Gütschow, G. Klebe, T. Steinmetzer, New 3-amidinophenylalanine-derived inhibitors of matriptase, Med Chem. Comm. 3 (2012) 807–813, https://doi.org/10.1039/C2MD20074K.
[22] E. Fliszár-Nyúl, Z. Faisal, V. Mohos, D. Derdák, B. Lemli, T. Kálai, C. Sár, B.Z. Zsidó, C. Hetényi, Á.I. Horváth, Z. Helyes, R. Deme, D. Bogdán, A. Czompa, P. Mátyus, M. Poór, Interaction of SZV 1287, a novel oxime analgesic drug candidate, and its metabolites with serum albumin, J. Mol. Liq. 333 (2021), 115945, https://doi.org/10.1016/j.molliq.2021.115945.
[23] T. Hu, Y. Liu, Probing the interaction of cefodizime with human serum albumin using multi-spectroscopic and molecular docking techniques, J. Pharm. Biomed. Anal. 107 (2015) 325–332, https://doi.org/10.1016/j.jpba.2015.01.010.
[24] Z. Faisal, B. Lemli, D. Szerencsés, S. Kunsági-Máté, M. Bálint, C. Hetényi, M. Kuzma, M. Mayer, M. Poór, Interactions of zearalenone and its reduced metabolites a-zearalenol and b-zearalenol with serum albumins: species differences, binding sites, and thermodynamics, Mycotoxin Res. 34 (2018) 269–278, https://doi.org/10.1007/s12550-018-0321-6.
[25] M. Poór, G. Boda, V. Mohos, M. Kuzma, M. Bálint, C. Hetényi, T. Bencsik, Pharmacokinetic interaction of diosmetin and silibinin with other drugs: inhibition of CYP2C9-mediated biotransformation and displacement from serum albumin, Biomed. Pharmacother. 102 (2018) 912–921, https://doi.org/10.1016/j.biopha.2018.03.146.
[26] V. Mohos, T. Bencsik, G. Boda, E. Fliszár-Nyúl, B. Lemli, S. Kunsági-Máté, M. Poór, Interactions of casticin, ipriflavone, and resveratrol with serum albumin and their inhibitory effects on CYP2C9 and CYP3A4 enzymes, Biomed. Pharm. 107 (2018) 777–784, https://doi.org/10.1016/j.biopha.2018.08.068.
[27] V. Mohos, E. Fliszár-Nyúl, O. Ungvári, É. Bakos, K. Kuffa, T. Bencsik, B.Z. Zsidó, C. Hetényi, Á. Telbisz, C. Özvegy-Laczka, M. Poór, Effects of chrysin and its major conjugated metabolites chrysin-7-sulfate and chrysin-7-glucuronide on cytochrome P450 enzymes and on OATP, P-gp, BCRP, and MRP2 Transporters, Drug Metab. Dispos. 48 (2020) 1064–1073, https://doi.org/10.1124/dmd.120.000085.
[28] S. Günther, P.Y.A. Reinke, Y. Fernández-García, J. Lieske, T.J. Lane, H.M. Ginn, F. H.M. Koua, C. Ehrt, W. Ewert, D. Oberthuer, O. Yefanov, S. Meier, K. Lorenzen, B. Krichel, J.D. Kopicki, L. Gelisio, W. Brehm, I. Dunkel, B. Seychell, H. Gieseler, B. Norton-Baker, B. Escudero-Pérez, M. Domaracky, S. Saouane, A. Tolstikova, T. A. White, A. Hänle, M. Groessler, H. Fleckenstein, F. Trost, M. Galchenkova, Y. Gevorkov, C. Li, S. Awel, A. Peck, M. Barthelmess, F. Schlünzen, P. Lourdu Xavier, N. Werner, H. Andaleeb, N. Ullah, S. Falke, V. Srinivasan, B.A. França, M. Schwinzer, H. Brognaro, C. Rogers, D. Melo, J.J. Zaitseva-Doyle, J. Knoska, G. E. Peña-Murillo, A.R. Mashhour, V. Hennicke, P. Fischer, J. Hakanpää, J. Meyer, P. Gribbon, B. Ellinger, M. Kuzikov, M. Wolf, A.R. Beccari, G. Bourenkov, D. von Stetten, G. Pompidor, I. Bento, S. Panneerselvam, I. Karpics, T.R. Schneider, M. M. Garcia-Alai, S. Niebling, C. Günther, C. Schmidt, R. Schubert, H. Han, J. Boger, D.C.F. Monteiro, L. Zhang, X. Sun, J. Pletzer-Zelgert, J. Wollenhaupt, C.G. Feiler, M.S. Weiss, E.C. Schulz, P. Mehrabi, K. Karničar, A. Usenik, J. Loboda, H. Tidow, A. Chari, R. Hilgenfeld, C. Uetrecht, R. Cox, A. Zaliani, T. Beck, M. Rarey, S. Günther, D. Turk, W. Hinrichs, H.N. Chapman, A.R. Pearson, C. Betzel, A. Meents, X-ray screening identifies active site and allosteric inhibitors of SARS-CoV-2 main protease, Science 372 (6542) (2021) 642–646, https://doi:10.1126/science.abf7945.
[29] L. Zhang, D. Lin, X. Sun, U. Curth, C. Drosten, L. Sauerhering, S. Becker, K. Rox, R. Hilgenfeld, Crystal structure of SARS-CoV-2 main protease provides a basis for design of improved α-ketoamide inhibitors, Science 368 (6489) (2020) 409–412, https://doi:10.1126/science.abb3405.
[30] D. Meyer, F. Sielaff, M. Hammami, E. Böttcher-Friebertshäuser, W. Garten, T. Steinmetzer, Identification of the first synthetic inhibitors of the type II transmembrane serine protease TMPRSS2 suitable for inhibition of influenza virus activation, Biochem J. 452 (2) (2013) 331–343, https://doi.org/10.1042/bj20130101.
[31] E. Colombo, A. Désilets, D. Duchêne, F. Chagnon, R. Najmanovich, R. Leduc, E. Marsault, Design and synthesis of potent, selective inhibitors of matriptase, ACS Med. Chem. Lett. 3 (7) (2012) 530–534, https://doi.org/10.1021/ml3000534.
[32] E. Pászti-Gere, J. Pomothy, Á. Jerzsele, O. Pilgram, T. Steinmetzer, Exposure of human intestinal epithelial cells and primary human hepatocytes to trypsin-like serine protease inhibitors with potential antiviral effect, J. Enzym. Inhib. Med. Chem. 36 (1) (2021) 659–668, https://doi.org/10.1080/14756366.2021.1886093.
[33] T. Steinmetzer, K. Hardes, E. Böttcher-Friebertshäuser, W. Garten, Strategies for the development of influenza drugs: basis for new efficient combination therapies, Top. Med Chem. 15 (2015) 143–182, https://doi.org/10.1007/7355_2014_84.
[34] E. Pászti-Gere, E. Czimmermann, G. Ujhelyi, P. Balla, A. Maiwald, T. Steinmetzer, In vitro characterization of TMPRSS2 inhibition in IPEC-J2 cells, J. Enzym. Inhib. Med Chem. 31 (Sup2) (2016) S123–S129, https://doi.org/10.1080/14756366.2016.1193732.
[35] D.A. Sychev, G.M. Ashraf, A.A. Svistunov, M.L. Maksimov, V.V. Tarasov, V. N. Chubarev, V.A. Otdelenov, N.P. Denisenko, G.E. Barreto, G. Aliev, The cytochrome P450 isoenzyme and some new opportunities for the prediction of negative drug interaction in vivo, Drug Des. Dev. Ther. 12 (2018) 1147–1156, https://doi.org/10.2147/DDDT.S149069.
[36] J. Stürzebecher, D. Prasa, J. Hauptmann, H. Vieweg, P. Wikström, Synthesis and structure-activity relationships of potent thrombin inhibitors: piperazides of 3-amidinophenylalanine, J. Med. Chem. 40 (19) (1997) 3091–3099, https://doi:10.1021/jm960668h.
[37] D. Gustafsson, R. Bylund, T. Antonsson, I. Nilsson, J.E. Nyström, U. Eriksson, U. Bredberg, A.C. Teger-Nilsson, A new oral anticoagulant: the 50-year challenge, Nat. Rev. Drug Discov. 3 (8) (2004) 649–659, https://doi:10.1038/nrd1466.
[38] C. Park, J.G. Ha, S. Choi, E. Kim, K. Noh, B.S. Shin, W. Kang, HPLC-MS/MS analysis of mesupron and its application to a pharmacokinetic study in rats, J. Pharm. Biomed. Anal. 150 (2018) 39–42, https://doi:10.1016/j.jpba.2017.12.002.
[39] J. Stürzebecher, H. Vieweg, T. Steinmetzer, A. Schweinitz, M.T. Stubbs, M. Renatus, P. Wikström, 3-Amidinophenylalanine-based inhibitors of urokinase. Bioorg. Med. Chem. Lett. 9 (21) (1999) 3147–3152, https://doi:10.1016/s0960-894x(99)00541-7.